Proceedings of the 2006 IASME/WSEAS International Conference on Energy & Environmental Systems, Chalkida, Greece, May 8-10, 2006 (pp293-298)

Numerical investigation of the buoyancy-induced flow field and heat transfer inside solar chimneys

E. BACHAROUDIS, M.GR. VRACHOPOULOS, M.K. KOUKOU, A.E. FILIOS

Mechanical Engineering Department, Environmental Research Laboratory
Technological Educational Institution of Chalkida
344 00 Psachna, Evia
HELLAS

Abstract: - A numerical investigation of the transport phenomena that take place inside a solar chimney is performed. The developed model faces the problem as a natural convection one between two vertical parallel plates. The governing elliptic equations are solved in a two-dimensional domain using a control volume method. Predicted velocity and temperature profiles are presented for different locations, at the inlet, at various internal points and at the outlet of the channel. Important parameters such as average Nusselt number are compared and calculated at several grid resolution. First results show that the model predicts realistically the system's behavior for various conditions.

Key-Words: - solar chimney, buoyancy-induced flow field, simulation

1 Introduction

The application of solar chimneys is an effective technique for reducing the temperature inside a building as well as for the provision of natural ventilation, which helps in lowering the humidity and achieving comfortable conditions inside the space. Its application in buildings may provide the required ventilation while simultaneously covers part of the heating and cooling requirements. The bouyancy-induced air flow depends on the difference in air density between the inside and outside of the solar chimney.

Solar chimneys have been investigated by a number of researchers and for different applications including passive solar heating and cooling of buildings, ventilation, power generation, etc. [1-4]. In the past, experimental and theoretical studies have been conducted for the determination of the size of solar chimneys, confirming that the velocity of air flow and temperature of different parts are functions of the gap between absorber and walls, ambient air temperature, and the elevation of air exit above the inlet duct.

Although the behavior of solar chimneys in their general form has been studied and certified both theoretically and experimentally, however, the wall solar chimney concept has not been certified at a laboratory level. To meet this objective experimental and theoretical work has been scheduled so as to obtain a clear understanding of the system's operation. At this stage of the on-going research work, a typical layout of a solar chimney has been simulated facing the problem as a natural convection one between two vertical parallel plates. The governing elliptic equations are solved in a two-dimensional domain using a control volume method. Predicted velocity and temperature profiles are presented for different locations, at the inlet, at various internal points and at the outlet of the channel. Important parameters such as average Nusselt number are compared and calculated at several grid resolution.

First results show that the model predicts realistically the system's behavior for various temperature conditions. The procedure is general and can be applied for the simulation of solar chimneys of different aspect ratios and conditions. Next steps include the customization of the developed model to describe the buoyancy-induced flow field in in-house developed wall solar chimneys that have been constructed in the Technological Educational Institution of Chalkida.

2 Problem Formulation

2.1 The physical problem

The study focuses on the vertical channel of the solar chimney and a numerical investigation of the natural buoyancy-driven fluid flow and the heat transfer in the vertical channel is attempted. In Figure 1 the geometry of the solar chimney is presented wherein L, is the height of the chimney and b, is the inter-plate spacing. Various cases have

been considered:

Case i) the channel's walls are isothermal and in the same temperature $T_{w1}=T_{w2}=T_w$
Case ii) the channel's walls are isothermal but in different temperatures $T_{w1}\neq T_{w2}$
Case iii) right wall is adiabatic.

In all the cases considered heat transfer through the walls causes buoyancy-driven flow. The chimney studied has 1m height (L) and 0.1m inter-plate spacing (b) and the channel aspect ratio is equal to $\frac{b}{L}=0.1$

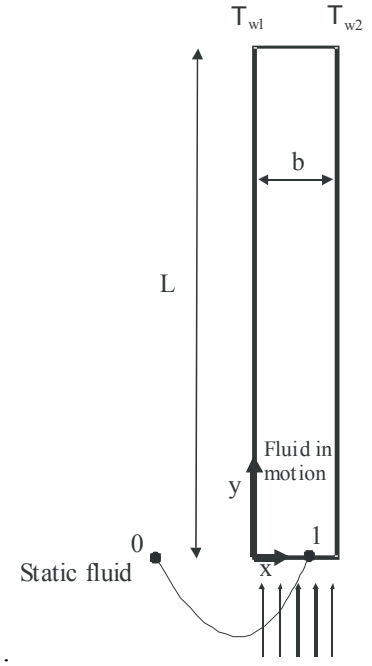

Fig. 1. The geometry studied

It is also assumed that outside the chimney the fluid is at rest. The solution of the governing conservation equations depends on the Rayleigh number based on the inter-plate spacing, Ra_b [5-6]:

$$Ra_b=\frac{g\beta(T_{w1}-T_o)b^3}{\nu^2}\cdot Pr \qquad (1)$$

where β, is the volumetric thermal expansion coefficient namely the change in the density of air as a function of temperature at constant pressure (K^{-1}), g is the gravitational acceleration ($9.81 m^2/s$), ν is the kinematic viscosity (m^2/s), T_{w1} is the left wall temperature and T_o, is the inlet air temperature.
The modified Rayleigh number based on inter-plate spacing is also used:

$$Ra^*=Ra_b\cdot\left(\frac{b}{L}\right) \text{ or } Ra^*=\frac{g\beta(T_{w1}-T_o)b^4}{\nu^2 L}\cdot Pr \quad (2)$$

An important characteristic of the flow is the rate of heat transfer through the solar chimney walls. Using Newton's law of cooling for the local convection coefficient h the Nusselt number for the left and right wall based on the inter-plate spacing of Figure 1 may be expressed as [5-6]:

Left wall:

$$Nu_{bl}=\frac{h\cdot b}{k},\quad h=\frac{q}{T_{w1}-T_o},q=\int\frac{\partial T}{\partial x}\Big|_{x=0}dy \quad (3)$$

Right wall:

$$Nu_{br}=\frac{h\cdot b}{k},\quad h=\frac{q}{T_o-T_{w2}},q=\int\frac{\partial T}{\partial x}\Big|_{x=0}dy \quad (4)$$

2.2 Mathematical model

2.2.1 The governing equations

A numerical investigation of the natural buoyancy-driven fluid flow and heat transfer in the vertical channel has been attempted. The simulations were conducted using the commercial, well-known, general-purpose CFD code, Fluent® [7]. The steady, laminar, incompressible and two-dimensional form of the equations of continuity, momentum and energy [5-9] was solved for the fluid flow in the vertical channel using the Boussinesq approximation [10]. The latter imposes constant values in all thermophysical properties except for the density in the buoyancy force term of the momentum equation. It is also assumed that viscous dissipation is neglected.

2.2.2 Boundary conditions

Boundary conditions have been specified at the inlet, outlet and walls of the solar chimney.

Inlet: At the inlet section, it is obvious that there is a specific velocity profile because the fluid is moving with a specific mass flow rate. It is well-known that this velocity profile is the result of the pressure difference between two points inside and outside of the channel at the same height. Let us consider the points 0, 1 in Figure 1. The fluid is motionless at the point 0 in ambient temperature $T_o=20^oC$ and static pressure p_o.

In point 1 the fluid obtains an unknown velocity profile which produces mass flow rate Q at inlet temperature T_o and static pressure p.
According to the literature [11-14] it is assumed that the air moves from point 0 to point 1 with an adiabatic and reversible way. Specifically the Bernoulli equation holds at the entrance region outside the channel and the pressure difference between the two points is converted to kinetic energy. From Figure 1 (Bernoulli $0 \to 1$):

$$\begin{aligned} & p + \frac{1}{2}\rho u^2 = p_o \Rightarrow \\ & p - p_o + \frac{1}{2}\rho u^2 = 0 \Rightarrow \\ & p' + \frac{1}{2}\rho u^2 = 0 \Rightarrow \\ & p' = -\frac{1}{2}\rho u^2 \end{aligned} \quad (5)$$

where: p', is the 'reduced' static pressure and $p_{o,}$ is the ambient pressure with $p_o = -\rho_o g y$. Moreover, it is assumed that the streamwise variations of temperature are neglected. Finally, under certain conditions, conduction effects at inlet could be important, but for Ra* in order of 10^5 it can be assumed that these are negligible.

Outlet:
At the outlet section the streamwise variations of velocity components and temperature are neglected. In addition, it is assumed that the fluid's pressure becomes equal to the ambient pressure [11-14].

It is well-known that static pressure in an arbitrary point can be written as: $p = p' + p_o \Rightarrow$
$p = p' - \rho_o g y$

In order to be satisfied the preceding condition $p = p_o$ at the outlet region, we have to impose $p' = 0$. In this way according to Gadafalch et al [12] all the kinetic energy of the air is assumed to be converted to heat. Finally, it was defined a Backflow Total Temperature=20°C in case the fluid entered to the chimney from the outlet. In this case we consider the incoming air to be fresh air in a temperature T_o=20°C.

Walls:
Case i) The walls of the chimney are isothermal and have both the same temperature equal to: $T_{w1}=T_{w2}$=40°C.
Case ii) The left wall temperature is isothermal and T_{w1}=40°C and the right wall temperature is isothermal and T_{w2}=30°C.
Case iii) The left wall temperature is isothermal and T_{w1}=40°C and the right wall is adiabatic.

Additional non-slip conditions for velocities are imposed at the channel walls.

2.2.3 Grid Independence

A structure, mapped mesh with quadrilateral 2D elements has been built in the code. In order to ensure the accuracy of the numerical results, a detailed grid independence study was performed by changing the number of the nodes in the horizontal (H) and in the vertical (V) direction (Table 1).
The purpose was to define the best mesh resolution to capture the boundary layer regime. In the simulations a grid with 40×80 quadrilateral cells has been used giving grid independent solutions for all the cases considered.

Table 1 Average Nusselt number Nu_{bl} for different grids.

V/H=2	Nu_{bl}	V/H=4	Nu_{bl}	V/H=6	Nu_{bl}
20×40	12.848	20×80	13.015	20×120	12.971
40×80	11.977	40×160	12.197	40×240	12.151
50×100	11.890	50×200	12.102	50×300	12.066
60×120	11.850	60×240	12.051	60×360	12.023
-	-	80×320	11.998	80×480	11.981

2.2.4 Numerical solution details

The solution of the set of the equations together with the boundary and internal conditions has been made with the segregated steady-state solver embodied in Fluent commercial software. Because the governing equations are non-linear (and coupled), several iterations of the solution loop must be performed before a converged solution is obtained.
For pressure-velocity coupling Fluent provides three methods in the segregated solver: SIMPLE, SIMPLEC, and PISO. SIMPLE has been used in all cases studied. Because of the non-linearity of the problem the solution process is controlled via relaxation factors that control the change of the variables as calculated at each iteration. The convergence is checked by several criteria (e.g. the conservation equations should be balanced; the residuals of the discretised conservation equations must steadily decrease).

3 Results and Discussion

In this section typical results from the performed simulations for the various cases considered are presented and discussed.

Case i) the channel's walls are in the same temperature $T_{w1}=T_{w2}=T_w$

The predicted mass flow rate for the solar chimney is $\dot{m}=0.0188\,\mathrm{Kg/s}$. For the validation of the results the empirical correlation of Zamora & Hernandez [14] for the average Nusselt number Nu_b number (based on the inter-plate spacing), b) with the modified Rayleigh Ra* was used [14]: $Nu_b=0.683(Ra^*)^{0.234}$. For $Ra^*=2{,}09\cdot10^5$ the last equation yields the average Nusselt for the boundary layer regime (Ra*>10^3): $Nu_b=12{,}004$.

The predicted average Nusselt number Nu_{bl} for the left wall based on inter-plate spacing is: $Nu_{bl}=12{,}018$ which is in excellent agreement with the previous value.

In Figures 2,3 the y velocity component and temperature profiles are presented. For Ra*>10^3, it is expected that the flow field in the channel approaches the boundary layer regime. Indeed, in Figures 2,3 the velocity and thermal boundary layers are created near the walls across the channel without interfere in each other.

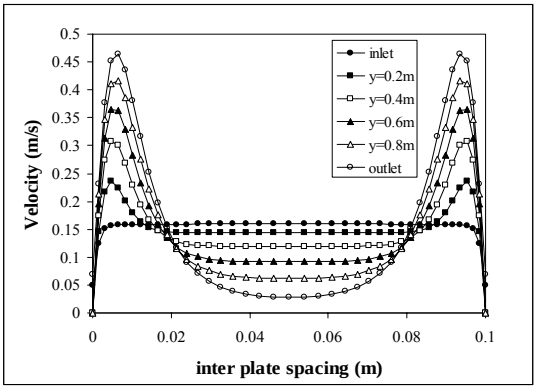

Fig. 2 Velocity profile vs inter plate spacing for various chimney heights. *Case i*

The shape of the velocity and temperature profile in different downstream sections almost coincides with the shape of the corresponding profile on a vertical flat plate. However, the problem of natural convection in a vertical channel for $Ra^*=2{,}09\cdot10^5$ even if it approaches the one in a vertical flat plate, is different and this fact is confirmed from the comparison between the numerical and the analytical solution in a vertical channel and in a vertical flat plate, respectively.

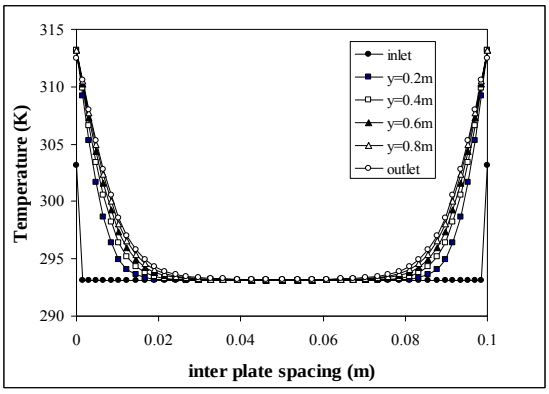

Fig. 3. Temperature profile vs inter plate spacing for various chimney heights. *Case i*

In Figure 4 the y velocity profile is presented in vector form at the outlet section, respectively. Two separated velocity boundary layers near the walls are noticed. The flow field is symmetric to the centerline of the channel as expected. Furthermore the velocity at the center of the duct has a small, constant value and it seems that no reverse flow take place in outlet region on such conditions. Close to the walls, in the thermal boundary layer, the flow is driven by buoyancy, and outside the thermal boundary layer it is driven by pressure forces resulting from the application of the pressure boundary condition at the inlet.

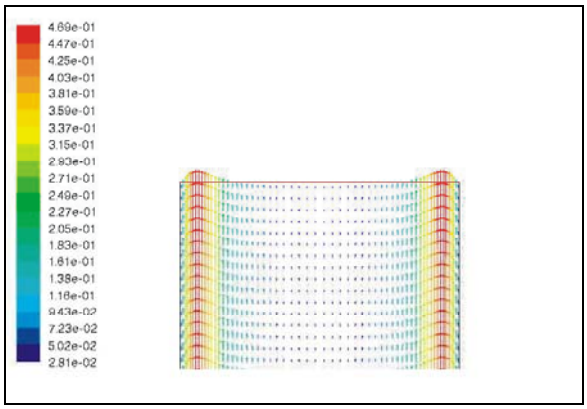

Fig. 4. Vectors of y-velocity component at the outlet region

Case ii) the channel's walls are in different temperatures $T_{w1}\neq T_{w2}$

The calculated mass flow rate for the solar chimney is $\dot{m}=0.0175\,\mathrm{Kg/s}$. The predicted average Nusselt number Nu_{bl} for the left wall based on the inter-plate

spacing is: $Nu_{bl} = 11{,}954$. The respected average Nusselt number for the right wall Nu_{br} based on the inter-plate spacing is: $Nu_{br} = 10{,}305$. In Figures 5,6 the y velocity component and temperature profiles are presented where the velocity and thermal boundary layers are created near the walls across the channel.

The two boundary layers are formed independently without interfere with each other. As the air moves up to the outlet of the vertical channel, the flow is being accelerated and two maxima are created near the heated walls. The flow field and temperature profile are not symmetric to the centerline of the channel as expected because of the difference between the two wall temperatures.

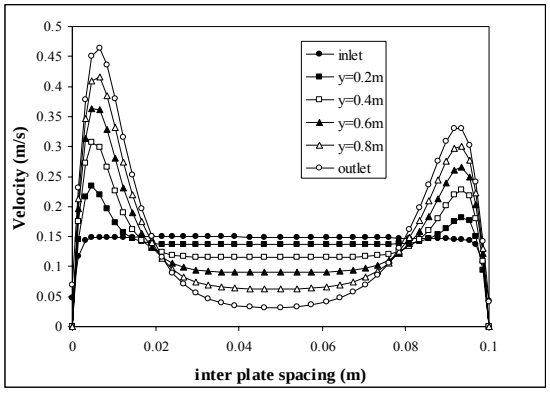

Fig. 5 Velocity profile vs inter plate spacing for various chimney heights. *Case ii*

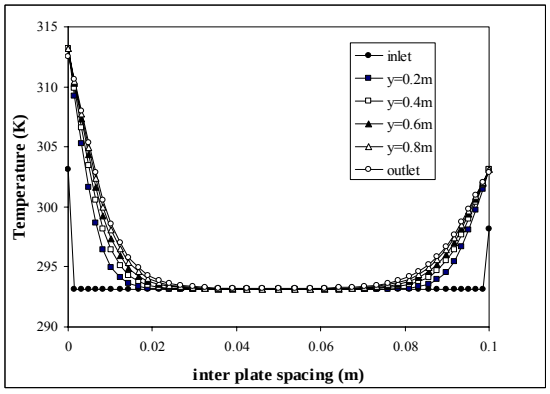

Fig. 6. Temperature profile vs inter plate spacing for various chimney heights. *Case ii*

Case iii) the right wall is adiabatic

The calculated mass flow rate for the solar chimney is $\dot{m} = 0.0067\,\mathrm{Kg/s}$. For the validation of the results the empirical correlation of Zamora & Hernandez for the average Nusselt number Nu_b number (based on the inter-plate spacing, b) with the modified Rayleigh Ra* was used [14]: $Nu_{bl} = 0.631(Ra^*)^{0.238}$. For $Ra^* = 2{,}09 \cdot 10^5$ the last equation yields the average Nusselt: $Nu_{bl} = 11{,}647$.

The predicted average Nusselt number Nu_{bl} for the left wall based on the inter-plate spacing is: $Nu_{bl} = 11{,}427$ which is in excellent agreement with the previous value.

Finally, in Figures 7,8 the y velocity component and temperature profiles are presented where the velocity and thermal boundary layers are created near the walls across the left wall channel.

An important remark is the reverse flow occurring from the middle of the solar chimney and upwards. The appearance of this recirculation region is easily explained. Since buoyancy pushes the flow towards the hot wall, new fluid needs to be admitted through the exit, in order to satisfy mass conservation. For the vertical channel the penetration depth of the reverse flow of 0.5L compares very well with the value of 0.46L observed experimentally [11].

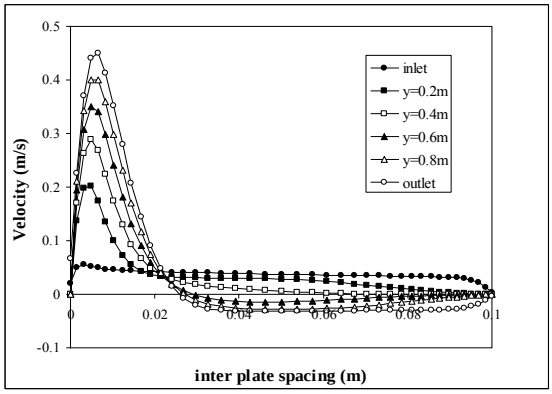

Fig. 7 Velocity profile vs inter plate spacing for various chimney heights. *Case iii*

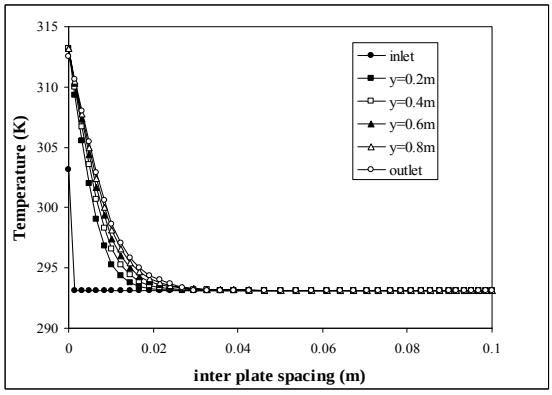

Fig. 8. Temperature profile vs inter plate spacing for various chimney heights. *Case iii*

4 Conclusion

In this work research focuses on the study of the thermofluid phenomena occuring inside solar chimneys. A numerical investigation of the buoyancy-driven flow field and heat transfer that take place inside solar chimneys is performed. The developed model faces the problem as a natural convection one between two vertical parallel plates.

The governing elliptic equations are solved in a two-dimensional domain using a control volume method. Predicted velocity and temperature profiles together with the average Nusselt number are presented for different locations, at the inlet, at various internal points and at the outlet of the channel. First results show that the model predicts realistically the system behaviour for various temperature conditions. The procedure is general and can be applied for the simulation of solar chimneys of different aspect ratios and conditions.

5 Acknowledgement

Authors would like to thank Hellenic Ministry of National Education and Religious Affairs and European Commission that financially supported this work under the auspices of the Operational Programme for Education and Initial Vocational Training, Archimedes Programme.

References:

[1] G. Gan, S.B. Riffat, A numerical study of solar chimney for natural ventilation of buildings with heat recovery, *Applied Thermal Engineering*, Vol. 18, 1998, pp. 1171-1187.

[2] C. Afonso, A. Oliveira, Solar chimneys: simulation and experiment, *Energy and Buildings*, Vol. 32, 2000, pp. 71–79.

[3] K.S. Ong, C.C. Chow, Performance of solar chimney, *Solar Energy*, Vol. 74, 2003, pp. 1–17.

[4] J. Khedari, N. Rachapradit, J. Hirunlabh, Field study of performance of solar chimney with air conditioned, *Energy and Buildings,* Vol. 28, 2003, pp. 1099–1114.

[5] J.P. Holman, Heat transfer, Fourth Edition, International Student Edition, 1976.

[6] B.R. Bird, W.E. Stewart, E.N. Lightfoot, *Transport phenomena*, John Wiley & Sons, Inc., New York, 1960.

[7] Fluent 6.1 User's Guide 2003.

[8] S.V. Patankar, *Numerical heat transfer and fluid flow*, McGraw Hill, New York, 1980.

[9] N.C. Markatos, K.A. Pericleous, Laminar and Turbulent Natural Convection in an Enclosed Cavity, *Int. J. Heat Mass Transfer*, Vol. 27 (5), 1984, pp. 755-772.

[10] D.D. Gray, A. Giorgini, The validity of the Boussinesq approximation for liquids and gases, *Int. J. Heat and Mass Transfer*, Vol. 19, 1976, pp. 545-551.

[11] F. Marcondes, C.R. Maliska, Treatment of the inlet boundary conditions in natural-convection flows in open-ended channels, *Numerical Heat Transfer Part B*, Vol. 35, 1999, pp. 317-345.

[12] A.S. Kaiser, B. Zamora, A. Viedma, Correlation for Nusselt number in natural convection in vertical convergent channels at uniform wall temperature by a numerical investigation, *International Journal of Heat and Fluid Flow*, Vol. 25, 2004, pp. 671-682.

[12] J. Gadafalch, A. Oliva, G. Van der Graaf, X. Albets, Natural convection in a large, inclined channel with asymmetric heating and surface radiation, *ASME Journal of Heat Transfer*, Vol. 125, 2003, pp. 812-820.

[13] G. Desrayaud, A. Fichera, Laminar natural convection in a vertical isothermal channel with symmetric surface-mounted rectangular ribs, *International Journal of Heat and Fluid Flow,* Vol. 23, 2002, pp. 519-529.

[14] B. Zamora, J. Hernandez, Influence of variable property effects on natural convection flows in asymmetrically-heated vertical channels, *International Communications in Heat and Mass Transfer*, Vol. 24, 1997, pp. 1153-1162.